Journal of Controlled Release 353 (2023) 51–62

Contents lists available at ScienceDirect

Journal of Controlled Release

journal homepage: www.elsevier.com/locate/jconrel

Insulin-loaded liposomes packaged in alginate hydrogels promote the oral bioavailability of insulin

Haishan Wu [a,b], Jian Nan [a,b], Liu Yang [a,b], Hyun Jin Park [c], Jinglei Li [a,b,*]

[a] School of Food and Biological Engineering, Hefei University of Technology, Hefei 230009, China
[b] Engineering Research Center of Bio-process, Ministry of Education, Hefei University of Technology, Hefei 230009, China
[c] School of Life Sciences and Biotechnology, Korea University, Seoul, Republic of Korea

ARTICLE INFO

Keywords:
Oral administration
Cysteine
Alginate
Intestinal absorption
Insulin

ABSTRACT

Compared to subcutaneous injections, oral administration of insulin would be a preferred route of drug administration for diabetic patients. For oral delivery, both liposomes and alginate hydrogels face many challenges, including early burst release of the encapsulated drug and poor intestinal drug absorption. Also, adhesion to the intestinal mucosa remains weak, which all result in a low bioavailability of the payload. This study reports on an alginate hydrogel loaded with liposomes for oral insulin administration. Liposomes (Lip) loaded with arginine-insulin complexes (AINS) were incorporated into a hydrogel prepared from cysteine modified alginate (Cys-Alg) to form liposome-in-alginate hydrogels (AINS-Lip-Gel). An *ex vivo* study proves that intestinal permeation of AINS and AINS-Lip is approximately 2.0 and 6.0-fold, respectively, higher than that of free insulin. The hydrogel retarded early release of insulin (~30%) from the liposomes and enhanced the intestinal mucosal retention. *In vivo* experiments revealed that the AINS-Lip-Gel released insulin in a controlled manner and possessed strong hypoglycemic effects. We conclude that liposome-in-alginate hydrogels loaded with AINS represent an attractive strategy for the oral delivery of insulin.

1. Introduction

Diabetes is a severe disease impacting nearly 10% of the whole population, which is still increasing in the predictable future due to the trend of population aging globally [1]. In the context of COVID-19 pandemic, it is imperative to pay more attention to diabetic patient management [2]. Hyperglycemia is a prominent trait of diabetes ascribed to delayed or insufficient insulin secretion. Metformin and many other drugs are usually prescribed to control the high blood glucose, which inevitably causes some side effects [3].

Insulin is still the most effective drug to control blood glucose levels, especially for severe diabetic management. Compared with injection, oral insulin administration is much preferred [4]. However, the gastrointestinal (GI) tract presents a hostile environment for oral insulin administration, accompanied with a strongly acidic environment (pH 1.2–2.0) and digestive enzymes, which significantly denature and degrade insulin and reduce its bioactivity [5]. The mucus lines on the surface of the GI tract and introduces a barrier against protein drugs like insulin. Effective adhesion and quick penetration of intestinal mucus are important for drugs to avoid elimination by the continuously secreted mucus [6].

To address these challenges, various types of carriers were applied to protect insulin against the harsh environment in the GI tract and improve its oral bio-efficacy. Liposome is a typical drug carrier that reduces systemic toxicity and improves tolerable doses [7]. Since the 1970s, liposomes with different properties have been developed as carriers for oral insulin administration [8]. However, conventional liposomes are destabilized in an acidic environment, leading to an early release of payloads and low bio-efficacy. To improve the release pattern and bio-efficacy, complicated modifications of liposomes are required which indeed restrict their practical applications for oral insulin administraiton.

Hydrogel is another extensively investigated carrier for insulin [9]. Hydrogel is a water-swollen 3D polymer network that contains a high amount of water but remains the structure owing to physical or chemical crosslinks, which resembles the extracellular matrix. Alginate (Alg) hydrogel is commonly considered as a biocompatible platform for oral insulin administration that is stable in an acidic environment [10]. A carrier that precisely coordinates the release kinetics of insulin in specific locations is critical for improving the bio-efficacy of insulin [11].

* Corresponding author at: School of Food and Biological Engineering, Hefei University of Technology, Hefei 230009, China.
E-mail address: lijinglei2012@hotmail.com (J. Li).

https://doi.org/10.1016/j.jconrel.2022.11.032
Received 14 May 2022; Received in revised form 11 November 2022; Accepted 16 November 2022
Available online 23 November 2022

However, the porous structure of Alg hydrogel leads to early burst release of payloads and poor intestinal absorption [12]. Besides, simple Alg hydrogel provides only weak adhesion to intestinal mucosa, offers a short residence time on the surface of the small intestine, and leads to a low absorption rate [13]. Hence, modified Alg hydrogel with stronger adhesion ability on the intestinal mucosa is promising for oral insulin administration.

A single type of carrier, such as liposome and hydrogel, usually focuses on specific problems of oral insulin administration, such as burst release in stomach, weak mucosal retention on the intestinal mucosa and low intestinal absorption [14–18]. In recent years, complex delivery platforms combining two or more carriers have proved more efficient as delivery tools. In our previous study, Alg microbeads were applied to load insulin-encapsulated chitosan nanoparticles for oral insulin administration [19]. Meanwhile, chitosan-based hydrogel was applied to incorporate chlorhexidine-loaded liposomes, which significantly improved the biofilm eradication ability [20]. Another study integrated different modular liposomes into the hydrogel to form a liposome-in-hydrogel complex delivery system as an injectable protein drug carrier [11]. Liposome-in-hydrogel combines the strength of both liposome and hydrogel as drug carriers and provides an effective solution for oral insulin delivery. However, to the best of our knowledge, there is still no report on using the liposome-in-hydrogel complex for oral insulin delivery.

Based on previous research and our understanding, we hypothesized that the liposome-in-alginate hydrogel complex is an effective delivery tool to encapsulate, protect, and promote the insulin absorption for oral administration.

In this study, we aim to develop a multi-functional oral delivery system for improving the bio-efficacy of insulin. As a proof of concept, the liposome-in-alginate hydrogel complex is designed as the delivery system. To promote intestinal permeation and absorption efficiency, instead of pristine insulin, an arginine-insulin complex was prepared by electrostatic attraction [21,22]. Liposome (Lip) was applied to encapsulate the arginine-insulin complex (AINS) to protect insulin and further improve intestinal permeation and absorption. Furthermore, instead of Alg, cysteine-modified alginate (Cys-Alg) was used to form hydrogel to improve the adhesive ability of the intestinal mucosa [13], which is beneficial to the absorption of Lip by the epithelial cells. Cys-Alg hydrogel avoids burst release of insulin from the Lip in an acidic environment. In the intestine, Cys-Alg hydrogel would swell and release the negatively charged Lip, which would be absorbed by intestinal cells. The oral bio-efficacy of insulin could be significantly improved.

2. Materials and methods

2.1. Materials

Insulin (derived from porcine pancreas), phosphatidylethanolamine, cholesterol, 5,5′-dithio bis-(2-nitrobenzoic acid), L-arginine, and L-cysteine hydrochloride were purchased from Aladdin (Shanghai, China). Sodium alginate (200 ± 20 mPa·s) was obtained from Macklin (Shanghai, China). All other reagents and cell culture materials were provided by Aladdin (Shanghai, China).

2.2. Preparation of liposome hydrogel complex oral delivery system

2.2.1. Preparation of arginine-insulin complex (AINS)

Insulin was fully dissolved in 0.01 M HCl solution. The pH value was adjusted to 7.6 by adding 0.1 M NaOH and 0.1 M phosphate buffer solution (PBS). Arginine (Arg) was dissolved in deionized water and mixed with insulin at different ratios of concentration (2:1, 2:3, and 1:3, mol/mol) to form an arginine-insulin complex (AINS-1, AINS-2, and AINS-3) with the pH value adjusted to 7.6. The size and PDI were measured by a Zetasizer Nano (Malvern, UK).

2.2.2. Synthesis of cysteine modified alginate (Cys-Alg)

Cysteine was grafted to alginate (Alg) through 1-(3-dimethylaminopropyl)-3-ethylcarbodiimide hydrochloride (EDC)/N-hydroxy succinimide (NHS)-mediated amidation reaction. Briefly, EDC and NHS powders were added into Alg solution with pH value adjusted to 5.5. The solution was incubated at a dark room temperature for 45 min. Then, L-cysteine hydrochloride was dissolved into the Alg solution with a pH value adjusted to 4.75. The reaction was continued at room temperature for 5 h. Unreacted cysteine (Cys) and small molecule impurity was dialyzed against 5 mmol/L HCl twice in the dark. HCl (5 mmol/L) containing 1% (*w/v*) NaCl was used to reduce the ionic exchange between cationic polymers and anionic sulfhydryl polymers. Finally, the mixed solution was dialyzed against 1 mmol/L HCl twice and freeze-dried after the pH value was adjusted to 4.0.

2.2.3. Preparation of AINS loaded liposome (AINS-Lip)

Thin film hydration method was used to prepare liposomes (Lip). The homogeneous lipid film was induced under vacuum in a round-bottom flask containing a chloroform solution of phosphatidylethanolamine and cholesterol (3:1, mol/mol). The film was hydrated by an arginine-insulin complex (AINS) solution for 30 min at room temperature, followed by 3 rounds of extrusion through a polycarbonate membrane with 0.22 μm pores.

2.2.4. Preparation of liposome-in-alginate hydrogel complex (Lip-Gel)

To encapsulate insulin-arginine complex loaded Lip (AINS-Lip), the freeze dried and weighted hydrogels were immersed in AINS-Lip solution at a concentration ratio of 1:20 and allowed to swell. The reaction was performed at 37 °C overnight. After swelling equilibrium, the AINS-Lip loaded hydrogels (AINS-Lip-Gel) were stored at 4 °C for further studies.

2.3. Characteristics

2.3.1. The dynamic light scattering (DLS) measurements

DLS measurements (size, polydispersity, and zeta potential) of AINS, AINS-Lip, and blank Lip were conducted by Zetasizer Nano (Malvern, UK) at 25 °C and a scattering angle of 90°.

2.3.2. Fourier transform infrared spectroscopy (FTIR) and nuclear magnetic resonance (NMR) analysis

Cys, Alg, and Cys-Alg were lyophilized and analyzed by ATR-FTIR on a PerkinElmer Spectrum 100 spectrophotometer (Waltham, MA, USA). The frequency range of ATR-FTIR between 600 cm^{-1} to 4000 cm^{-1} and a resolution of 4 cm^{-1} with 16 scans were applied. Alg, Cys, Cys-Alg, and cystine alginate physical mixture were dissolved in deuterium oxide (D_2O) to measure the ^1H nuclear magnetic resonance (NMR) spectra on an Agilent VNMRS600 600 Hz ^1H NMR instrument.

2.3.3. Quantification of crosslinking ratio and the thiol group content

The content of carbon, hydrogen, oxygen, nitrogen, and sulfur in Cys-Alg and alginate were measured by an elemental analyzer (Vario EL, Elementar, Germany) [23]. According to the atomic composition of the Cys-Alg and Alg, the crosslinking ratio is calculated by the following formula:

$$\%\text{crosslinking ratio} = \frac{\%Cys}{\%Alg} = \frac{\%S(conjugate-Alg)/32}{\%C(Alg)/72}$$

Where %S means the atomic percentage of sulfur, and %C means the atomic percentage of carbon.

The thiol group content in Cys-Alg was determined by the 5,5′-dithiobis-2-nitrobenzoic acid (DTNB) reagent. Cys-Alg (4 mg) was dissolved into 1 mL demineralized water with a pH value adjusted to 4.0 by 0.1 M HCl solution. After that, Cys-Alg was mixed with DTNB solutions and reacted at room temperature for 15 min in the dark. The absorption at 412 nm was recorded on an ultraviolet spectrophotometer.

2.3.4. Transmission electron microscope (TEM) and field emission scanning electron microscopy (SEM) observation

The morphology of blank Lip and AINS-Lip were observed by TEM (1200EX, Japan). Lip and AINS-Lip were diluted 100 times and loaded on a copper grid. Both Lip and AINS-Lip were stained by phosphotungstic acid solution (2%) and washed with demineralized water. For SEM observation, Lip-Gel was swollen to equilibrium at different pH values (2.0, 4.0, and 6.8), followed by freezing in liquid nitrogen. The samples were stored at −80 °C overnight and lyophilized. The conductivity of lyophilized hydrogels was improved by coating with gold [24]. After that, the morphology of the Lip-Gel was observed by SEM (Regulus 8230, Japan).

2.3.5. The encapsulation efficiency (EE) and loading capacity (LC)

The encapsulation efficiency (EE) and loading capacity (LC) were determined according to the previous method [25]. After preparation, the pH value of the AINS-Lip solution was adjusted to 7.4 and centrifuged at 18000*g* for 30 min to remove AINS-Lip. The content of unloaded insulin was measured by reversed-phase high- performance liquid chromatography (RP-HPLC, E2695, Waters, USA) on a C18 column (5 μm, 4.6 × 250 mm) equipped with Waters 2998 UV/visible detector operated at 25 °C. Acetonitrile and TFA aqueous solution (0.1%) at a ratio of 30:70 (*v*/v) was used as the mobile phase. The flow rate of eluent was 0.8 mL/min. Insulin was detected at the wavelength of 214 nm. EE and LC were calculated using the following eqs.

$$EE\% = \frac{\text{the amount of total insulin} - \text{the amount of free insulin}}{\text{the amount of total insulin}} \times 100\%$$

$$LC\% = \frac{\text{the amount of total insulin} - \text{the amount of free insulin}}{\text{the weight of NPs}} \times 100\%$$

2.4. In vitro experiments

2.4.1. Insulin release profile from Lip and Lip-Gel

To determine the release profile of insulin from Lip and Lip-gel at pH 1.2 and 6.8, AINS-Lip and AINS-Lip-Gel were pre-incubated at 37 °C, pH 1.2 (0.1 M HCl) and 6.8 (0.1 M PBS) solution continuously. An equal volume of sample solution was taken at the predetermined time intervals and centrifuged at 18000*g* for 20 min. The released amount of insulin was measured by the reversed-phase high-performance liquid chromatography (RP-HPLC, E2695, Waters, USA) [16].

2.4.2. Cell culture

Caco-2 cells were cultured in Dulbecco's modified eagle medium (DMEM), containing 1% nonessential amino acid, 1% L-glutamine, 1% streptomycin (100 IU/mL), and penicillin (100 IU/mL), and 10% fetal bovine serum, incubated at 37 °C in a humidified atmosphere of 5% CO_2.

2.4.3. Cell cytotoxicity

As biocompatibility is a crucial characteristic for long-term oral delivery, the cytotoxicity of hydrogels was tested by the 3-(4,5-dimethyl-2-thiazolyl)-2,5-diphenyl-2H-tetrazolium bromide (MTT) assay [26]. Caco-2 cells were seeded into a 96-well plate at a cell density of $3*10^4$/mL and incubated for 24 h to allow attachment. Then, the DMEM medium was renewed and different concentrations of AINS-Lip-Gel (0, 30, 60, 120, 250, 500, 1000, 2000, and 4000 μg/mL) were added into wells. PBS solution was used as a control. After that, the DMEM medium was removed from each well, followed by PBS washing three times. MTT was dropped into wells to form formazan crystals dissolved by dimethyl sulfoxide. The cell viability was determined by measuring the absorbance at 570 nm on a microplate reader.

2.4.4. Cellular uptake

Caco-2 cells were used to investigate the cellular uptake of AINS-Lip and AINS-Lip-Gel. Caco-2 cells were cultured according to the previous protocol. Cells were grown in a 24-well plate at a density of $1*10^4$ cells/well and cultured for 24 h. FITC- labeled insulin (FITC-INS) was prepared according to the previous method [27]. DMEM medium was removed, and Caco-2 cells were incubated with FITC-AINS (FITC-labeled insulin) loaded liposome (FITC-AINS-Lip) and FITC-AINS-Lip-Gel at 40 μg/mL (concentration of FITC-INS) respectively. The concentration of FITC-Lip-Gel was 4 mg/mL. After 3 h of incubation, formulations were removed, and the cell nuclei were stained with Hoechst 33342. The samples were imaged using a confocal laser scanning microscope (CLSM, Zeiss, German) [28]. The macroscopic appearance of FITC-AINS-Lip-Gel incubated with DMEM medium was also recorded at different time intervals in triplicate.

2.5. Animals experiments

2.5.1. Animals care

All animal protocols were approved by the Animals Ethics Committee of Hefei University of Technology and conducted according to the guide for laboratory animals. Female Institute of Cancer Research (ICR) mice (6–8 weeks, 16–18 g) were purchased from Anhui Medical University, maintained at standard SPF-class laboratory conditions with 7 days light/dark cycle, and used for the following experiments.

2.5.2. Absorption studies of the ligated intestinal loops

The qualitative absorption of FITC-INS, FITC-AINS, and FITC-AINS-Lip solutions in ileum villus of rats was investigated by the ligated intestinal loops model *in vivo* [29]. Male Sprague-Daley (SD) rats were fasted but allowed free access to water overnight before experiment. SD rats were anesthetized *via* intraperitoneal injection of chloral hydrate, and then different formulations were injected into 3-cm sections of ileum loops. After one hour, the loops were cut off and extensively washed with PBS solution. Afterwards, the small intestinal tissue-sections were prepared. The absorption of formulations by intestinal tissues was observed by confocal laser scanning microscope (CLSM).

2.5.3. Retention on intestinal mucosa

The mucosal retention of FITC-INS in the presence of Lip and Lip-Gel was evaluated by fluorescence microscopy based on a previous method with slight modifications [30]. Fresh intestinal tissues were obtained from male SD rats. The contents of the small intestine were washed with preheated PBS (37 °C). The small intestine was cut open and placed on a 75 × 25 mm glass slide with the mucosal side facing upward. After that, 100 μL of different formulations were added to the surface of intestinal mucosa. Meanwhile, images were recorded before and after each washing cycle with preheated PBS solution delivered by a peristaltic pump (BT-200B, Shanghai).

2.5.4. Ex vivo intestinal permeation

Ileum is widely used as a simple model to study drug permeation profiles in the intestine [29]. In order to further quantitatively determine the intestinal permeation ability, 4-cm ileum tissues were cut off from sacrificed rats to prepare ligated intestinal loops. Thereafter, 0.4 mL of FITC-INS, FITC-AINS, FITC-AINS-Lip, and FITC-AINS-Lip-Gel were injected into intestinal loops, which were incubated in 10 mL Krebs'-Ringer buffer solution at 37 °C with low-speed stirring. At different time intervals (0.5, 1, 2, 3 h), 400 μL volume of Krebs'-Ringer buffer solution was taken away and renewed by the same volume of Krebs'-Ringer buffer solution [25]. The amount of transported FITC-INS was measured by a fluorospectrophotometer in triplicate. The apparent permeability coefficient (P_{app}) was calculated by the following equation

$$Papp = \frac{dQ}{dt} * \frac{1}{A*C}$$

where, *dQ/dt* is the flux rate of FITC-INS from ligated intestinal loop to Krebs'-Ringer buffer solution, A and C represent the surface area of

ligated intestinal segments and the initial concentration of FITC-INS in ligated intestinal segments, respectively.

2.5.5. Decrease of thiol groups

As the sulfhydryl group of cysteine is easily oxidized to form disulfide bonds, the decrease of thiol group was used to reflect the change of cross-linking degree in Cys-Alg hydrogel. The content of thiol group was measured in PBS solution (pH 6.8, containing 0.9% NaCl) at 37 °C because thiol group only oxidize in basic and neutral conditions. In brief, 40 mg Cys-Alg was incubated in 10 mL of PBS solution at 37 °C, under stirring [13]. At predetermined time intervals, a 50 μL sample was taken immediately for further analysis. The same volume of PBS solution was added to the Cys-Alg solution. The amounts of remaining thiol groups in Cys-Alg at different time intervals were determined as described in Section 2.3.3.

2.5.6. In vivo hypoglycemic experiments

Diabetic mice model was induced by continuous subcutaneous injection of streptozotocin (STZ, 50 mg/kg) for five days. Mice were fasted overnight before STZ injection. Mice with blood glucose levels above 16.7 mmol/L were chosen as diabetic model for further experiments [17]. Diabetic mice were divided into five groups ($n = 6$), including positive control (subcutaneous injection of insulin, 2 IU/kg), AINS and AINS-Lip group (orally administered at a dose of 60 IU/kg), AINS-Lip-Gel group (orally administered at a dose of 40 IU/kg) and 0.9% normal saline for oral administration as a blank control. The blood glucose levels were recorded by a glucose meter. Mice were fasted overnight before the intervention with free access to water.

2.6. Statistical analysis

The data were analyzed by two tail student's *t*-test and one-way ANOVA. All the experiments were conducted in triplicate except for the additional description. All the data were shown as means ± standard deviation, and the statistically significant difference means $p<0.05$.

3. Results

3.1. DLS, TEM, FITR and NMR analysis

The size distribution and surface charge of Lip, AINS-Lip, and AINS were measured by dynamic light scattering (DLS). As insulin aggregation affects its bio-efficacy, the influence of arginine on insulin aggregation was preliminarily investigated [31]. The sizes of AINS-1, 2, and 3 are 14.7, 12.5, and 10.4 nm, respectively, while the PDIs are 0.41, 0.32, and 0.33, respectively. DLS result reveals that there is no significant difference among different AINS groups. A previous study reported that a higher arginine concentration could promote intestinal insulin absorption; hence the AINS-3 was chosen for the following experiments [32]. The size distribution of Lip mainly ranged from 80 to 200 nm, while the insulin-loaded Lip ranged mostly from 100 to 300 nm (Fig. 1a and b). The zeta-potential of Lip and AINS-Lip were − 50.2 and − 22.8 mV, respectively. The zeta potential value of Lip increased after AINS loading, which is ascribed to the lower absolute value of AINS. TEM images demonstrated that Lip and AINS-Lip were small in size (<200 nm), corresponding with the DLS result (Fig. 1c and d). The encapsulation efficiency and loading capacity of Lip were 75.9% and 20.2%, respectively.

FTIR spectrometer was used to characterize the molecular structures of Alg, Cys, and Cys-Alg (Fig. 1e). After the thiolation of alginate, new bands appeared at 3284, 1631.1 and 1563.2 cm^{-1}, which represent the stretching vibrations of N—H bonds, C═O bonds in the amide, stretching vibrations of C—N bonds and wagging vibrations of NH bonds in the CH_2-NH-CH- group, respectively [33–35]. The new sharp band at 1724.3 cm^{-1} is the stretching vibration of unreacted -COOH in Cys. Band at 1248.0 cm^{-1} is the stretching vibration of C—N bonds and bending vibrations of N—H bonds in the amide [33]. Additionally, the characteristic peak of thiol group is weakly present at 2500 cm^{-1} in the spectrum of Cys-Alg, indicating the existence of Cys [36]. For ^1H NMR spectrum, the new peak around 2.9 ppm and peak at 3.8 ppm represents methylene and protons α-carbon, respectively, in Cys, which verified the successful thiolated modification (Fig. 1f) [37,38]. The above results indicate that the Cys was successfully conjugated to sodium alginate.

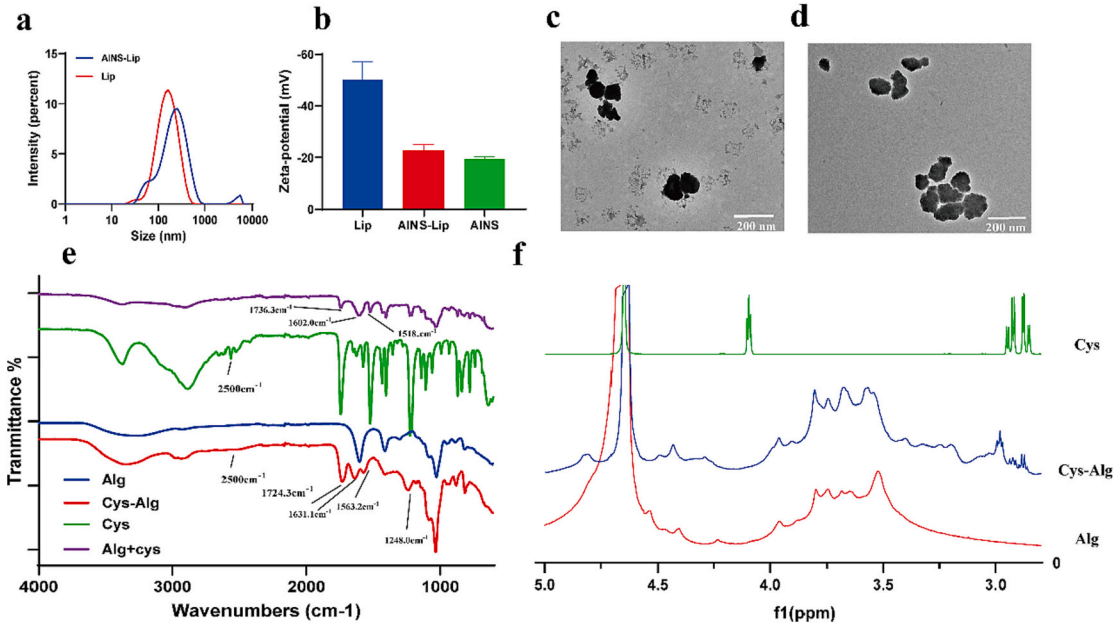

Fig. 1. Representative characterization of liposome (Lip) and modified alginate. (a) Images showing the distribution of particles size of Lip and arginine-insulin complex (AINS) loaded liposome (AINS-Lip); (b) zeta-potential of Lip, AINS-Lip and AINS; (c-d) morphology of Lip and AINS-Lip respectively, scale bar is 200 nm; (e) Fourier transform infrared spectroscopy (FTIR) spectra of alginate (Alg), L-cysteine hydrochloride (Cys), physical mixture of Alg and Cys (Cys + Alg) and Cys-Alg conjugate (Cys-Alg); (f) ^1H NMR spectra of hydrochloride (Cys), alginate (Alg) and Cys-Alg conjugate (Cys-Alg) respectively.

3.2. Quantification of the thiol group content and crosslinking ratio

The cross-linking ratio was deduced from the elemental composition of Cys-Alg backbone, especially the percentage of nitrogen and sulfur contained in cross-linkers. The crosslinking degree of Cys-Alg-1, Cys-Alg-2, and Cys-Alg-3 was 5.0%, 5.5%, and 6.2%, respectively (Table 1), showing no significant difference. However, during the preparation, we noticed that the appearance of spongy products of various samples after lyophilization was very different. Cys-Alg-3 exhibited a stronger texture and an uneven appearance, indicating that the composition of modified polymer is not evenly distributed in the polymer. Meanwhile, the appearance of Cys-Alg-2 was more homogeneous than Cys-Alg-1. Based on above results, the Cys-Alg-2 (the concentration ratio of insulin and arginine is 1:3) was used for further experiments.

Subsequently, the content of thiol group was determined in Cys-Alg-2 by the DTNB method. The crosslinking ratio (mol%) is 5.2% according to this method. The two methods showed a slight difference. The possible reason is that the content of thiol groups is partly disrupted by the reduction of the sulfhydryl of cysteine during preparation and storage, resulting in a lower crosslinking ratio as determined by the DTNB method.

3.3. SEM observation

To observe the morphological change of hydrogel and incorporated Lip under different pH conditions, the pH value of Lip-Gel solution was equilibrated at pH 1.2, 4.0 (the original value), and 6.8, respectively, before lyophilization. SEM images indicate that all the hydrogels exhibited a 3-dimensional feature with pore structures (Fig. 2d-f). Nevertheless, the pore size of hydrogels varied significantly under different pH conditions. At pH 4.0, hydrogel structure appeared similar and porous, with pore sizes mainly ranging around 30 μm. By comparison, the structure of Lip-Gel collapsed inward and exhibited smaller pore sizes varying 5–20 μm with lower porosity at pH 1.2, ascribed to the mostly protonated alginate and lower crosslinking degrees. At pH 6.8, the polymer backbone was partially protonated, leading to larger pore sizes ranging from 50 to 100 μm. Under this condition, Lip or released insulin was more likely to be divorced from hydrogel. Collectively, the SEM results indicated that Lip-Gel is pH-sensitive, which shrinks its crosslinking network in an acidic environment and swells to bigger pore sizes at pH 6.8. Besides, the morphology of Lip in the hydrogel was also clearly observed (Fig. 2a-c). The appearance of Lip was polyhedron instead of regular spherical shape, which presented bigger size than that revealed in TEM images, ascribed to the acidic condition. Based on the SEM observation, the distribution of Lip in hydrogel was further confirmed by Bruker X Flash 60 EDS to locate phosphorus element. SEM-EDS revealed that the red color (phosphorus element) was evenly distributed on the surface of the 3-dimensional structure of hydrogel (Fig. 2g-i). Phosphorus element was not detected in the Cys-Alg hydrogel contains no liposomes, which eliminates the possibility of unspecific background (Fig. S1). The above result reveals that Lip were enclosed in the hydrogel matrix, which can change its crosslinking degrees, pore sizes, and porosity at different pH values.

3.4. In vitro experiments

3.4.1. Insulin release from Lip-Gel and Lip

The release profile of AINS-Lip and AINS-Lip-Gel was measured at pH 1.2 and 6.8 respectively. At pH 1.2, after releasing for 3 h, the percentage of released insulin from Lip was around 40%, while the value was 10% for Lip-Gel (Fig. 3b). The result indicated that AINS-Lip-Gel could effectively avoid 30% of initial burst insulin release from AINS-Lip in an acidic environment. DLS result suggested that the size of AINS-Lip increased from ~160 nm to ~1600 nm, which verified the structural change of AINS-Lip. However, the amount of released insulin from Lip and Lip-Gel at pH 6.8 showed no significant difference, which was 22.3% and 25.0%, respectively. The size of Lip also showed little changes. The appearance of Cys-Alg hydrogel was significantly different from under investigated pH values (Fig. S2a). Microsphere particles were produced at pH 1.2. But the hydrogel was totally swollen during the same incubation period at pH 6.8. The pH response property of hydrogel is reversible that lower pH (1.2) precipitate the hydrogel which was fully dissolved in solution with higher pH (6.8) (Fig. S2b). The structure of AINS-Lip-Gel is swollen at pH 6.8, losing the ability to retain AINS-Lip. Meanwhile, the negatively charged AINS-Lip could be repelled from hydrogel as the structure of hydrogel swells. After releasing for 6 h, the percentage amount of released insulin from AINS-Lip and AINS-Lip-Gel was 60% and 35.8%, respectively. Collectively, AINS-Lip-Gel retards the burst release of insulin from AINS-Lip in acidic conditions and accelerates the release in solutions with higher pH values.

3.4.2. Cell cytotoxicity

AINS-Lip-gel was assessed for cytotoxicity to Caco-2 cells, which is widely employed for studying drug transportation *via* intestinal tissue. MTT assay was conducted on Caco-2 cells after 48 h of co-incubation with AINS-Lip-Gel at various concentrations. Hydrogel at all tested concentrations (0–4 mg/mL) presented cell viability higher than 90% (Fig. 7a). Therefore, the cytocompatibility data strongly indicates that AINS-Lip-Gel has negligible cytotoxicity.

3.4.3. Cell uptake

The cellular uptake of AINS-Lip and AINS-Lip-Gel was investigated, respectively. To investigate whether the internal AINS-Lip could be absorbed by Caco-2 cells, FITC-AINS-Lip-Gel and FITC-AINS-Lip were incubated with Caco-2 cells, respectively. Besides, the macroscopic appearance of FITC-AINS-Lip-Gel during incubation was also recorded (Fig. S3). Hydrogel was added to cell culture at 4 mg/mL to avoid any possible damage to cells. The yellow color represents FITC-INS and reflects the outline of FITC-AINS-Lip-Gel. The yellow FITC-AINS-Lip-Gel was entirely immersed in culture medium at the beginning, and then the outline diffused and became weaker in the following hours. After 5 h, the whole outline of FITC-AINS-Lip-Gel was hardly observed in culture medium, which means that the structure of Lip-Gel was entirely swollen. CLSM determined the cellular uptake of FITC-AINS-Lip and FITC-AINS-Lip-Gel by Caco-2 cells after incubation with Caco-2 cells for 3 h. Overlay merged signal of the green fluorescence (FITC-INS) and blue fluorescence (cell nuclei) in FITC-Lip group suggests that Lip was absorbed by Caco-2 cells (Fig. 4b). Meanwhile, the green fluorescence signal in FITC-Lip-Gel group was weaker compared with Lip group, which means lower numbers of Lip were absorbed by Caco-2 cells. The results implied that the inner Lip could not be released from hydrogel immediately, which is likely to be ascribed to the relatively high viscosity and swelling properties of hydrogel.

Table 1
The formulation of hydrogels with different crosslinker contents.

No.	Alginate (mg)	Cysteine (mg)	EDC (mg)	NHS (mg)	crosslinking ratio (mol%)	Thiol group content (mmol/L)
Cys-Alg-1	100	20	57	29	5.0%	/
Cys-Alg-2	100	40	116	58	5.5%	1.0
Cys-Alg-3	100	60	170	87	6.2%	/

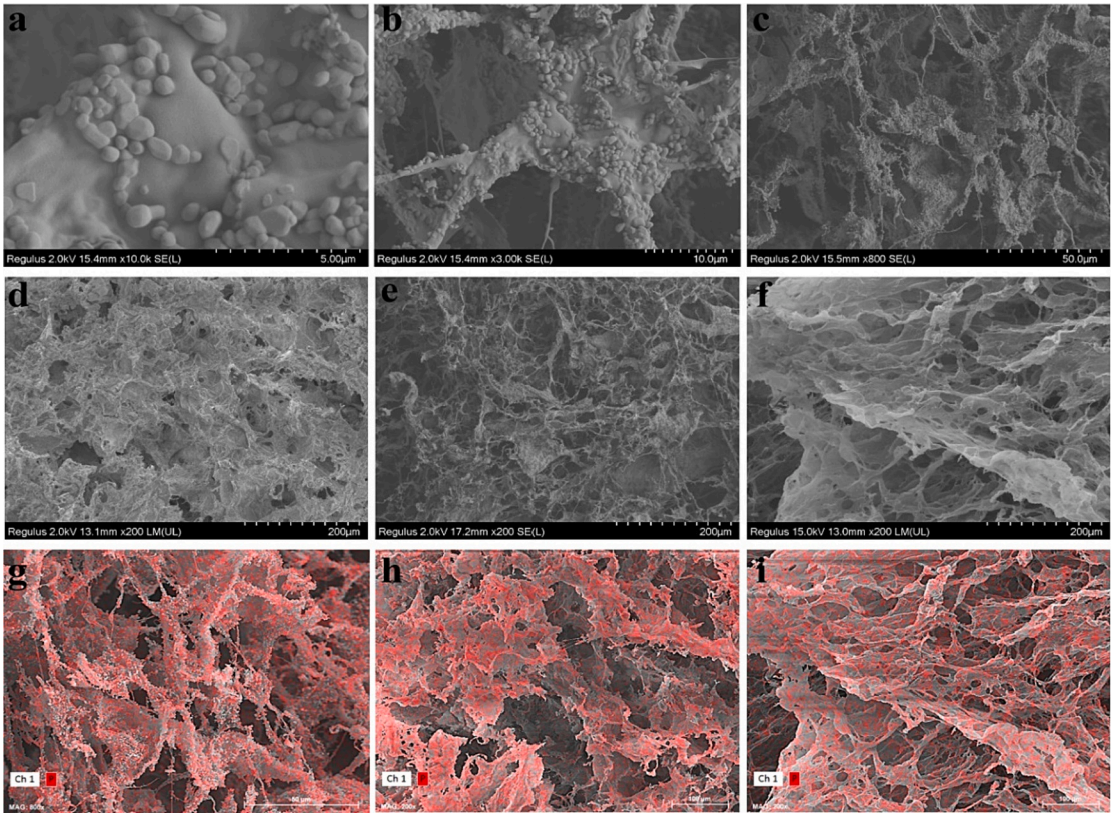

Fig. 2. The morphology of liposome loaded cysteine-alginate hydrogel (Lip-Gel) at different pH value. (a-c) Liposome in Lip-Gel, the scale bar represents 5, 10 and 50 μm respectively; (d-f) the morphology of crosslinking structure of Lip-Gel at pH 1.2, 4.0 and 6.8 respectively; (g-i) the distribution of phosphorus element, which are corresponding with the figure d-f.

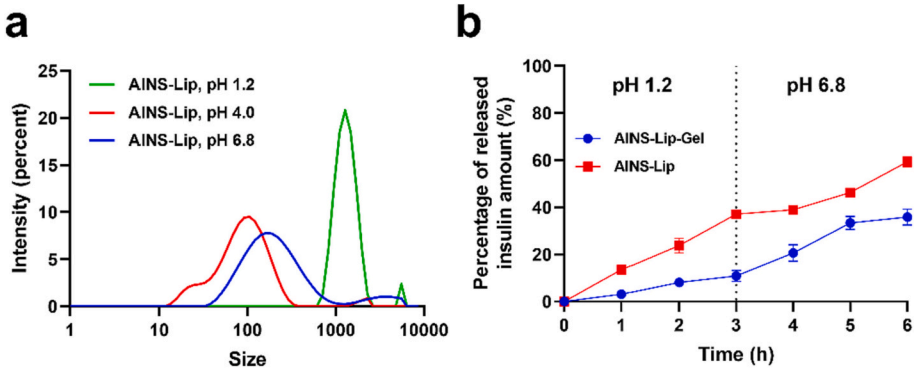

Fig. 3. The release profile of insulin from arginine-insulin loaded liposome (AINS-Lip) and AINS-hydrogel (AINS-Lip-Gel) at different pH value. (a) The size distribution of AINS-Lip at pH 1.2, 4.0 and 6.8 ($n = 3$); (b) the release profile of insulin from AINS-Lip and AINS-Lip-Gel at pH 1.2 and 6.8.

3.5. Animals experiments

3.5.1. Retention on intestinal mucosa

To investigate the mucosal retention ability, FITC-AINS-Lip was incorporated into the unmodified alginate and cysteine modified alginate hydrogel, respectively, before the experiments. The mucosal retention of Cys-Alg and Alg hydrogels was quantified according to the average fluorescence intensity (AFI), which was calculated by software image J. After washing with 10 mL of PBS, the AFI value of Cys-Alg and Alg retained in the intestinal mucosa was 24.3 and 14.6, respectively (Fig. 5a), showing a significant difference between Cys-Alg and Alg. In order to further investigate the mucosal retention ability, a higher washing speed of PBS solution was applied. After being washed with 50 mL PBS solution for one cycle, the Cys-Alg group showed a high AFI value of 109.3, while the Alg group was only 13.7 (Fig. 5b). The two experiments were conducted separately, using different batches of animal gut tissue samples. Notwithstanding, the AFI value of Cys-Alg and Alg groups presented no discrepancy after another wash cycle. The results vividly implied the stronger mucosal retention ability of Cys-Alg than Alg hydrogel.

3.5.2. Absorption studies in the ligated intestinal loops

In order to qualitatively analyze the influence of different formulations on intestinal absorption, FITC-INS, FITC-AINS, and FITC-AINS-Lip solutions were injected into ligated intestinal loops and observed by CLSM. After incubating in ligated intestinal loops for the same time, different formulations showed distinguishing absorption properties in intestinal tissue. Generally, continuously secreted mucus of high

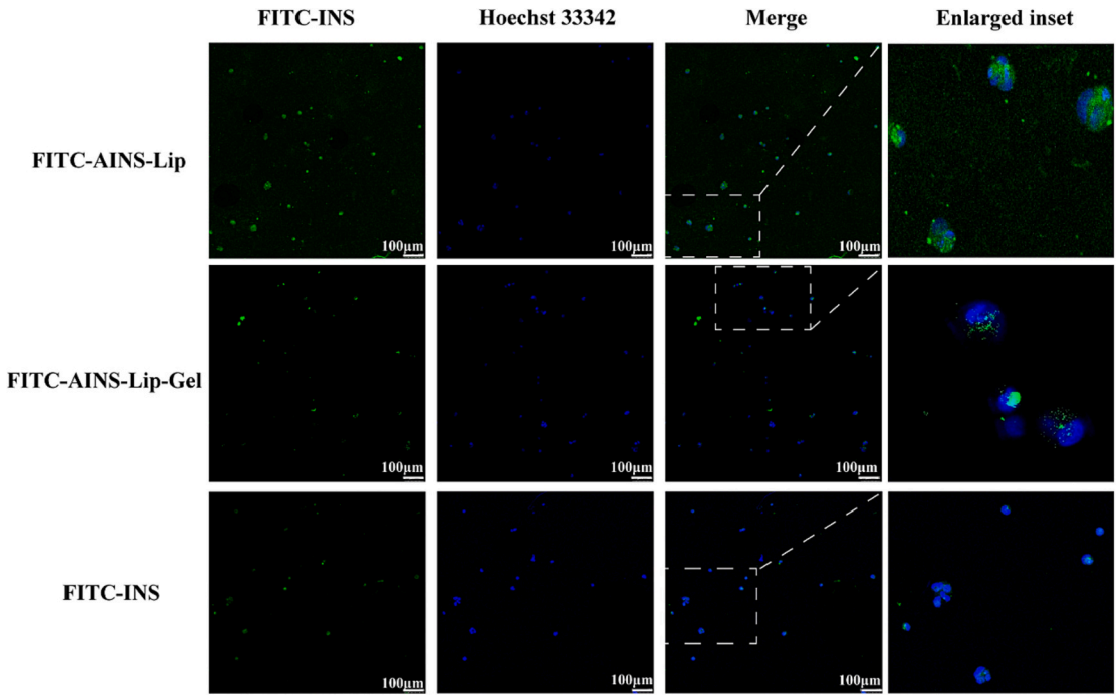

Fig. 4. Trans-epithelial cells transport of FITC labeled insulin (FITC-INS), FITC-loaded liposome (FITC-AINS-Lip) and AINS-Lip-hydrogel (FITC-AINS-Lip-Gel). The blue fluorescence is cell nucleus strained by Hoechst 33342, the green fluorescence is insulin strained by FITC. The first column represents the green fluorescence from insulin stained by FITC. The second column represents the blue fluorescence from the cell nuclei stained by Hoechst 33342. The third column represents the merged images corresponding to the first, and second images. Scale bars: 100 μm. The fourth column represents enlarged merge images of FITC-INS, FITC-AINS-Lip and FITC-AINS-Lip-Gel. (For interpretation of the references to color in this figure legend, the reader is referred to the web version of this article.)

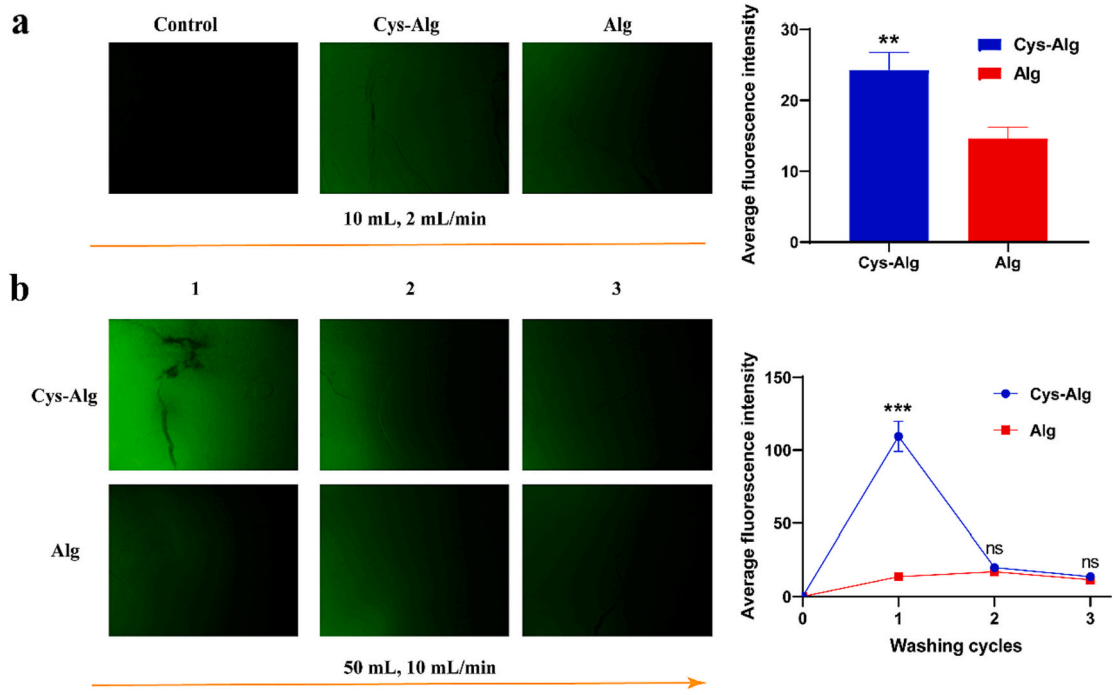

Fig. 5. Mucosal retention characteristic of cysteine modified alginate conjugate (Cys-Alg) and unmodified alginate (Alg) hydrogels. (a-b) Example microphotographs of hydrogels with washing speed of 2 mL/min (a) and 10 mL/min (b) at predetermined time intervals, with the average fluorescence intensity of different photos analyzed by software image J ($n = 3$). The small intestine tissues without the formulations was set as a control *p means statistically significant difference compared to Alg (**p<0.01 and ***p<0.001).

viscosity, negatively charged mucin and various enzymes form a strong barrier for extraneous matters, leading to slow and limited intestinal absorption [39]. Therefore, nanocarriers possess mucus-permeation property is promising for intestinal absorption. For the FITC-AINS group, a higher amount of insulin reached and absorbed by epithelial cells compared with the FITC-INS group at the same time, revealing that

the combination of arginine and insulin promotes the intestinal uptake of insulin (Fig. 6). After AINS was encapsulated by Lip, the intestinal tissue showed the strongest fluorescence among all groups. The result indicates that Lip significantly improves the intestinal uptake of insulin compared with other groups.

3.5.3. *In vitro intestinal permeation*

The permeation efficiency of INS, AINS, AINS-Lip, and AINS-Lip-Gel in ileum was determined by the *ex-vivo* method. The amounts of transported insulin (FITC labeled) from different groups exhibited obvious time-dependent traits (Fig. 7c). For free insulin solution, the cumulative level of transported INS increased from 98.8 to 231.4 ng/mL ($P_{app} = 4.1 \times 10^{-7}$ cm/s), while AINS solution showed approximately 2.0-fold (from 209.3 to 535.6 ng/mL, $P_{app} = 9.5 \times 10^{-7}$ cm/s) as that of INS group. Likewise, the AINS-Lip group also appeared to have 6.0 and 2.5-fold intestinal permeation (from 359.7 to 1437.6 ng/mL, $P_{app} = 2.5 \times 10^{-6}$ cm/s) compared with INS and AINS groups, respectively. Nevertheless, the AINS-Lip-Gel group exhibited the lowest amount of transported insulin (376.83 ng/mL, $P_{app} = 6.7 \times 10^{-7}$ cm/s), which was close to the value of AINS-Lip group at 0.5 h. As described in 3.5.3, the swollen process and high viscosity of Cys-Alg hydrogel retard the release of AINS-Lip. Besides, the formation of disulfide bonds within the thiolated polymer itself by reduction of the sulfhydryl increases the viscosity and retards the speed of swelling [13]. Accordingly, the formation of disulfide bonds was investigated by measuring the remaining thiol groups (Fig. 7b). The remaining thiol groups decreased to 67.9% after 2 h and reached 60.7% after 5 h.

3.5.4. *Hypoglycemic experiments*

In order to verify the hypoglycemic ability, diabetic model mice were treated with different formulations. The blood glucose levels were monitored after mice were fastened overnight (Fig. 8). Following the subcutaneous insulin injection, the blood glucose levels of mice sharply decreased within 2 h. After that, the glucose level rebounded quickly and returned to a level similar to that of the normal saline group. Insulin administrated by injection potently decreases the blood glucose level in a short period of time but lacks long-term effectiveness. In normal saline group the blood glucose of mice also decreased after 4 h, which is ascribed to the long-term fasten for 12 h [40]. Blood glucose levels of mice in the AINS-Lip group continuously decreased for 12 h. Oral administration of AINS-Lip showed a strong hypoglycemic effect, demonstrating that Lip can significantly improve the bio-efficacy of insulin. After 2 h of administration, AINS-Lip reaches the stomach and swells in the gastric juice, leading to a burst release of AINS. Small amount of insulin should avoid degradation and be absorbed by small intestine to exert a hypoglycemic effect. AINS group displayed similar tendency to the AINS-Lip group but showed a weak hypoglycemic effect, which corresponds with the results of intestinal absorption. In the preliminary experiment, the AINS-Lip-Gel at an insulin dose of 60 IU/kg caused severe hypoglycemia in mice. So, the dosage was decreased to 40 IU/kg for AIN-Lip-Gel. For oral AINS-Lip-Gel administration, the blood glucose levels of mice showed a slight drop and were kept in a flat state within 4 h, which indicated that a tiny amount of insulin was released from hydrogel or absorbed by intestinal tissue. AINS-Lip-Gel reached the small intestine after 3–4 h of administration. When reached to the small intestine, the hydrogel structure begun to disintegrate which leads to release of liposome and absorption of insulin. Meanwhile, the blood glucose level of AINS-Lip group was lower compared with AINS-Lip-Gel, which is corresponds with the result of different release profiles, cell uptake, and intestinal absorption *ex vivo* that showed a small amount of insulin was transported from AINS-Lip-Gel group within first 3 h. After that, the blood glucose levels sharply and continuously decreased from 4 h to 12 h, suggesting that a large amount of insulin was absorbed by intestinal cells and then reached the bloodstream. It is worth noticing that the hypoglycemic effect of AINS-Lip-Gel (40 IU/kg) and AINS-Lip (60 IU/kg) was similar, meaning AINS-Lip-Gel has higher insulin bio-efficiency compared with AINS-Lip.

In terms of relative pharmacological availability (PA%), AINS-Lip-Gel exhibited stronger hypoglycemic effect (PA of 11%), while the PA of AINS-Lip and AINS were 7% and 1%, respectively (Table 2). Recent publications only achieved 1–2% bioavailability for oral peptide bioavailability relative to s.c. administration, in line with our result

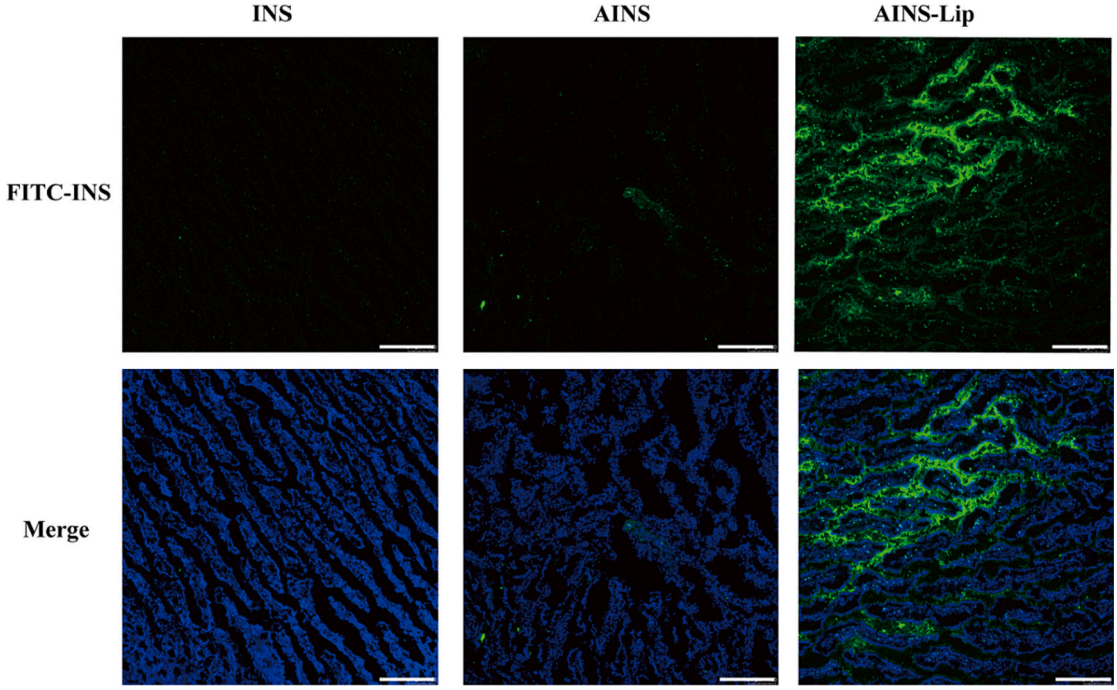

Fig. 6. Localization of FITC labeled insulin (FITC-INS), arginine-FITC labeled insulin (FITC-AINS) and FITC-AINS loaded Liposome (FITC-AINS-Lip) in villi of ileum after 1 h of incubation. Green fluorescence refers to the cell nucleus, and green fluorescence refers to FITC signal. (For interpretation of the references to color in this figure legend, the reader is referred to the web version of this article.)

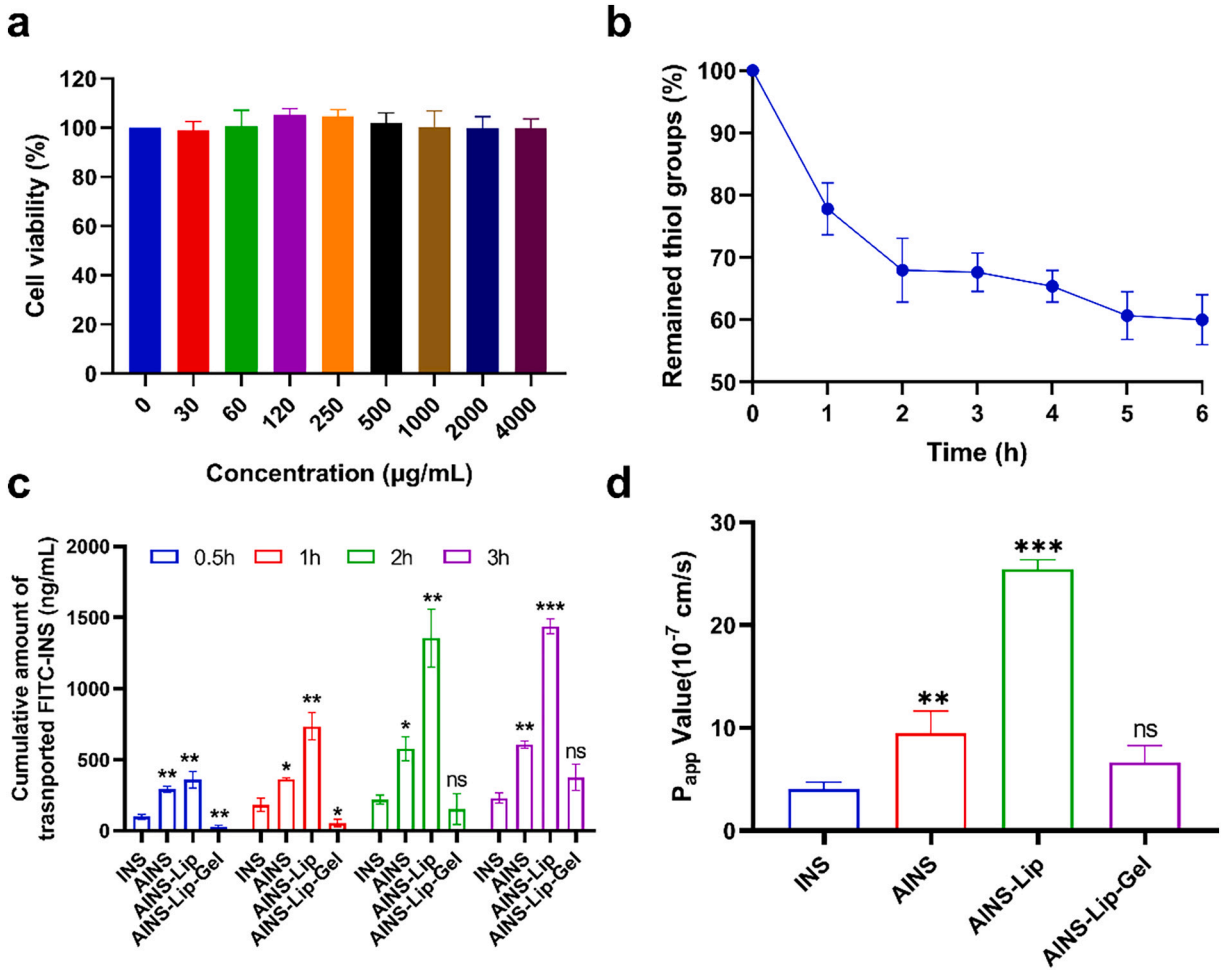

Fig. 7. The cell cytotoxicity test, intestinal permeation of FITC labeled insulin and reduction of thiol groups. (a) Effects of treatment with AINS-Lip-Gel on cell viability of Caco-2 cells for 48 h; (b) decrease in thiol groups within Cys-Alg incubated in PBS solution containing 0.9% NaCl (means±SD, $n = 3$); (c) accumulative permeated amount of insulin across rat ileum from INS, AINS, AINS-Lip and AINS-Lip-Gel (means±SD, n = 3); (d) P_{app} of INS, AINS, AINS-Lip and AINS-Lip-Gel in ileums (means±SD, n = 3). *p means statistically significant difference compared to INS group (*$p<0.05$, **$p<0.01$ and ***$p<0.001$).

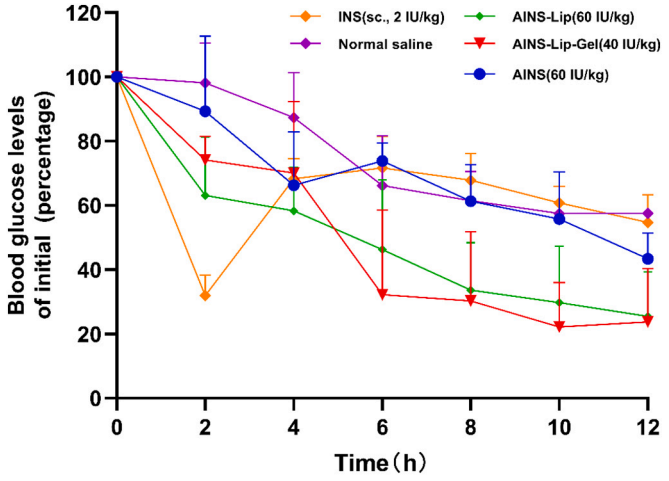

Fig. 8. Percentage change of initial blood glucose level of fasted diabetic mice treated by insulin, (s.c. 2 IU/kg), normal saline and different insulin loaded formulations (AINS (60 IU/kg), AINS-Lip (60 IU/kg) and AINS-Lip-Gel (40 IU/kg)) by oral administration (mean ± SD, $n = 6$).

Table 2
Relative pharmacological availability of different treatments in diabetic mice ($n = 6$).

Formulations	Insulin (s.c., 2 IU/kg)	AINS-Lip-Gel (40 IU/kg)	AINS-Lip (60 IU/kg)	AINS (60 IU/kg)
Dose [IU/kg]	2	40	60	60
AAC[a] [mmol/L·h]	143	317.5	311.2	62.3
PA[b] [%]	/	11%	7%	1%

[a] Area above the curve;
[b] Relative pharmacological availability.

[41]. Collectively, the above results indicate that oral AINS-Lip-Gel and AINS-Lip administration both present hypoglycemic effects, while the former displays stronger and continuous effects. *In vivo* results correspond with release profile and intestinal absorption. After oral Lip-Gel administration, hypoglycemic effects began at 4 h and remained for the last 8 h.

4. Discussion

The oral insulin administration can be traced back to 1922. In 2006, Pfizer introduced the first insulin inhaled formulation called Exubera, but it failed due to the high variation in insulin absorption, the complex

inhalation technique, and the low patient acceptance [42]. Therefore, designing an effective oral insulin delivery system is quite challenging but important for better diabetes management.

In the present study, we developed a novel oral delivery system for insulin. Insulin was combined with arginine to form a complex and then encapsulated by liposome (AINS-Lip). After that, AINS-Lip was embedded into Cys-Alg hydrogel. Arginine modification enhances the intestinal absorption of insulin. Liposome encapsulation increases stability and promotes the intestinal absorption of insulin. Cys-Alg hydrogel reduces insulin release in the stomach and prolongs mucosal retention in intestine. To prove the concepts, we thoroughly determined the characterization of the complex delivery system and studied the performances of various formulations under different pH conditions, intestinal retention, absorption, and hypoglycemic ability *in vivo*.

AINS-Lip possesses a small size (~160 nm and PDI<0.3) with a negative surface charge and high encapsulation efficiency (~75%). Generally, the size of a carrier below 500 nm with a neutrally or negatively charged surface promotes the penetration of mucus, which is highly related to intestinal absorption [43]. Therefore, the surface characteristics of AINS-Lip represent good traits for intestinal absorption. Reverse phase evaporation is the most preferred method for loading a hydrophilic drug such as insulin, leading to a yield of up to 30–50% [44,45]. The high encapsulation efficiency of AINS-Lip means less insulin was lost during sample preparation. Notably, TEM and SEM results revealed that Lip and AINS-Lip have polyhedron shapes instead of even spherical shapes. Lipids such as lysophosphatidylcholine and polyphosphoinositides tend to self-assemble and form curved monolayers, with surfaces bulging towards the polar heads and positive spontaneous curvature. Conversely, the monolayers formed by phosphatidylethanolamine and diacylglycerol possess a surface bulge in the direction of the hydrocarbon chains, leading to a cone-like shape with a negative spontaneous curvature [46]. Therefore, the shape of liposome was impacted by the lipid composition, which is related to the structures and energies of the propensity of lipid bilayers.

Liposome is unstable in the GI tract, which poses a challenge for retaining the bio-efficacy of insulin. Conventionally, phatidylethanolamine was employed to prepare pH-sensitive liposomes, which are stable at physiological pH [47]. At a lower pH value, protonation of phospholipid increases the angle of the head and tail group, inducing payload release [48]. After being embedded into Cys-Alg hydrogel, the amount of released insulin decreased by 75% (from 40% to 10%). By comparison, cyclodextrin complexed insulin encapsulated in hydrogel microparticles and poly (lactic-*co*-glycolic acid)- hydrazine bond-polyethylene glycol nanoparticles released 15% and 35% of insulin, respectively, in the same releasing period [17,49]. Interestingly, alginate is insoluble at lower pH but can form hydrogels *via* hydrogen bonding in an acidic medium. It is speculated that the 'egg-box' structure of Cys-Alg hydrogel shrank at pH 1.2 ascribed to protonated alginate, which enhanced the retaining ability of inner AINS-Lip. Meanwhile, the phospholipid bilayer of Lip becomes more tightly packed laterally at lower pH, inducing more negative spontaneous curvature of opposing monolayer and increasing the size of AINS-Lip [50]. The structural synergy of hydrogel and AINS-Lip resulted in the low release level of insulin from AINS-Lip-Gel, demonstrating its protection function to insulin. Besides, insulin at pH 1.2 presents a positive electric charge, attracted to the negatively charged alginate matrix, which results in a tighter structure of AINS-Lip-Gel.

The cellular uptake of AINS-Lip and AINS-Lip-Gel were also investigated, respectively. AINS-Lip promotes insulin absorption by Caco-2 cells. The inner AINS-Lip is not immediately released from the hydrogel, which is ascribed to the relatively high viscosity and swelling properties of hydrogel. Hydrogels tend to delay the release of incorporated carriers. The relatively high viscosity of AINS-Lip-Gel retards the diffusion of the incorporated AINS-Lip. Therefore, the absorption performance of AINS-Lip and AINS-Lip-Gel were discrepant. Besides, the cell cytotoxicity proved the high biocompatibility of AINS-Lip-Gel.

Retention of the intestinal mucosa is a prerequisite for insulin absorption by epithelial cells. Continuously secreted mucus could clear the carrier with poor ability of adhesion. Alginate hydrogel provides only weak interaction with mucus based on non-covalent bonds such as ionic interactions, hydrogen bonds, and van der Waal's forces. Therefore, cysteine modification introduced sulfhydryl groups into the alginate to enhance interaction with mucus and prolong mucosal retention. Cys-Alg showed stronger mucosal retention ability than that of simple Alg hydrogel. The formation of additional disulfide bonds between Cys-Alg polymer and mucus increases the mucoadhesive properties of Cys-Alg. The viscosity of the mucus/polymer interface is directly related to the mucoadhesive properties of the polymer. Higher mucoadhesive ability of Cys-Alg hydrogel is likely due to the presence of thiol groups in Cys, which promotes the formation of additional disulfide bonds with mucus [30]. The mucus glycoproteins contain abundant positively charged groups originating from amino acids, including arginine and lysine, which are located vicinal to Cys [51]. Besides, as mucus is neighbored by negatively charged -COO^- groups of Cys-Alg, the formation of disulfide bonds with thiol groups are highly favored. Therefore, the mucus is more likely to form additional disulfide bonds with the thiolated polymer Cys-Alg, resulting in stronger mucosal retention [13]. In addition, thiolated nanoparticles interact with mucin and further decrease the viscosity of mucus, which promotes mucus penetration and intestinal absorption of insulin, providing an additional pathway to overcome the challenges of intestinal transportation [52].

Intestinal absorption is a vital step for oral insulin delivery. Generally, continuously secreted mucus of high viscosity, negatively charged mucin, and various enzymes form a strong barrier for extraneous matters, leading to slow and poor intestinal absorption [39]. The intestinal absorption qualitatively and quantitatively was further investigated better to predict the fate of the carrier *in vivo*. AINS-Lip significantly improves the intestinal uptake of insulin compared with other groups, while AINS shows a weak effect. AINS presents approximately 2.0-fold as that of the INS group. Meanwhile, AINS-Lip group exhibits 6.0 and 2.5-fold intestinal permeation compared with INS and AINS groups, respectively. Insulin can bind strongly with oligoarginine to form a complex by electrostatic interaction, which increases its resistance against enzymes in intestine [53]. Furthermore, it can bind to the proteoglycans located at the cell surface, such as chondroitin sulfate and heparan sulfate [54]. The insulin-proteoglycan complex is internalized into epithelial cells *via* energy-independent pathways and partial endocytosis [55]. Therefore, arginine modification promotes the intestinal permeation of insulin. Arginine promotes the intestinal absorption of insulin, but lacks the necessary protection against chemical and enzymatic degradation. The negatively charged AINS-Lip avoids electrostatic bonding with mucus, reduces the capture in mucus, and thus promotes mucus penetration. As a phospholipid-based vesicle, Lip improves the solubility and stability of payload, protects insulin from inactivation, excretion, and enzymatic degradation, and thus preserves the potency of insulin [56]. Besides their higher resisting ability against protease, negatively charged liposomes could escape the endosomal and lysosomal degradation, as they can disrupt the negatively charged endosomal membrane by avoiding electrostatic interaction to form ion pairs [57]. Therefore, AINS-Lip exhibits the highest amount of transported insulin. The formation of disulfide bonds within the thiolated polymer leads to the stronger structural crosslinking of AINS-Lip-Gel. The higher degree of crosslinking leads to the tighter structure of AINS-Lip-Gel, slowing down the diffusion speed of Lip and retards the speed of swelling [13]. Therefore, lower numbers of Lip reached epithelial cells within the same period, leading to a smaller amount of transported insulin in AINS-Lip-Gel. However, due to the limitation of the *ex vivo* experiment, the AINS-Lip-Gel in the intestines of rats will not fully swell, which remains its strong crosslinking structure, and retards liposomes and insulin release. The intestinal environment of hydrogel will not reflect the actual scenario as a much smaller amount of hydrogel enter the intestine each time. Therefore, the *ex vivo* intestinal absorption

of hydrogel will reflect a much-delayed effect for AINS-Lip-Gel.

For insulin s.c. injection, many studies have shown that it is highly effective and only lasts for a short period of time [28,29]. Oral AINS-Lip administration displays stronger and continuous *in vivo* hypoglycemic ability with higher PA (7%) than insulin *via* s.c. injection, while AINS represented low PA (1%) ascribed to the poor protective effect in the GI tract, which could lead to insulin devitalization. Besides the benefit of reducing insulin release in the stomach and enhancing intestinal adhesion, a lower dosage of AINS-Lip-Gel (40 IU/kg) exhibited a similar hypoglycemic effect compared with AINS-Lip (60 IU/kg). Although AINS promotes intestinal transportation, it provides weak protection to insulin. Meanwhile, AINS-Lip provides specific protection and promotes intestinal insulin absorption, but its bio-efficiency is still very low. Thanks to the strong protection function of hydrogel, liposomes further improve the bio-efficiency of insulin, and reduce the dosage of insulin at the same time. It is not easy to simply adjust the insulin dose to improve the therapeutic efficacy of AINS-Lip-Gel, which could lead to hyperglycemia. There are two cutting-edge pathways to address this problem. One is to design an intelligent carrier system that responds to the concentration of glucose and releases insulin, which avoids the hyperglycemia and hypoglycemia ascribed to the insulin dose. Another one is combining blood glucose concentration with deep learning algorithms to develop a system that predicts the concentration of blood glucose in real-time and releases a certain dose of insulin to provide a safer and controllable pattern to avoid hyperglycemia and hypoglycemia.

5. Conclusions

In order to improve the stability and intestinal absorption of insulin for oral administration, a promising liposome-in-alginate hydrogel delivery system was developed and thoroughly investigated. Arginine was combined with insulin, encapsulated by liposome, and finally embedded in cysteine-modified alginate hydrogel named AINS-Lip-Gel. Insulin-loaded liposomes have a small size with a narrow distribution pattern. FITR, NMR, elemental analysis, and thiol group content all verified the existence of cysteine in the polymer backbones of Cys-Alg. The Cys-Alg hydrogel presents significant pH-sensitive release property. The structure of hydrogel shrinks and avoids the burst release of insulin from the Lip in a severe acidic environment. After the modification of cysteine, the mucosal retention of Alg hydrogel is improved by enhancing the interaction of the polymer with mucosa. The AINS-Lip also shows outstanding properties of cellular uptake and intestinal transportation. Both AINS-Lip and AINS-Lip-Gel demonstrate a significant and continuously hypoglycemic effect. However, the AINS-Lip-Gel displays controlled release behavior and a stronger hypoglycemic effect than AINS-Lip. Collectively, this oral delivery system provides a promising platform to protect insulin during digestion, promote intestinal transportation and absorption, and ultimately improve its oral bio-efficacy.

Funding sources

This work is supported by National Natural Science Foundation of China (31700015), Fundamental Research Funds for the Central Universities (JZ2018HGTB0244) and Anhui Natural Science Foundation (1808085QC66).

Declaration of Competing Interest

The authors declare no competing financial interests.

Data availability

Data will be made available on request.

Appendix A. Supplementary data

Supplementary data to this article can be found online at https://doi.org/10.1016/j.jconrel.2022.11.032.

References

[1] A. Ps, A. Ip, A. Ps, A. Bm, A. Sk, B. Nu, C. Sc, D. Lg, E. Aam, F. Ko, Global and regional diabetes prevalence estimates for 2019 and projections for 2030 and 2045: results from the International Diabetes Federation Diabetes Atlas, 9 th edition, Diabetes Res. Clin. Pract. 157 (2019), 107843.
[2] S. Lim, J.H. Bae, H.S. Kwon, M.A. Nauck, COVID-19 and diabetes mellitus: from pathophysiology to clinical management, Nat. Rev. Endocrinol. 17 (2021) 11–30.
[3] R. Libianto, T.M. Davis, E.I. Ekinci, Advances in type 2 diabetes therapy: a focus on cardiovascular and renal outcomes, Med. J. Australia. 212 (2020) 133–139.
[4] S. Satake, M.C. Moore, K. Igawa, M. Converse, B. Farmer, D.W. Neal, A. D. Cherrington, Direct and indirect effects of insulin on glucose uptake and storage by the liver, Diabetes 51 (2002) 1663–1671.
[5] A. Banerjee, K. Ibsen, T. Brown, R. Chen, C. Agatemor, S. Mitragotri, Ionic liquids for oral insulin delivery, P. Natl. Acad. Sci. USA. 115 (2018) 7296–7301.
[6] H. Wu, T. Guo, J. Nan, L. Yang, G. Liao, H.J. Park, J. Li, Hyaluronic-acid-coated chitosan nanoparticles for insulin oral delivery: fabrication, characterization, and hypoglycemic ability, Macromol. Biosci. 22 (2022) 2100493, https://doi.org/10.1002/mabi.202100493.
[7] Š. Koudelka, J. Turánek, Liposomal paclitaxel formulations, J. Control. Release 163 (2012) 322–334.
[8] G. Dapergolas, G. Gregoriadis, Hypoglycæmic effect of liposome-entrapped insulin administered intragastrically into rats, Lancet. 308 (1976) 824–827.
[9] K. Chaturvedi, K. Ganguly, M.N. Nadagouda, T.M. Aminabhavi, Polymeric hydrogels for oral insulin delivery, J. Control. Release 165 (2013) 129–138.
[10] B. Sarmento, D. Ferreira, F. Veiga, A. Ribeiro, Characterization of insulin-loaded alginate nanoparticles produced by ionotropic pre-gelation through DSC and FTIR studie, Carbohyd. Polym. 66 (2006) 1–7.
[11] S. Correa, A.K. Grosskopf, J.H. Klich, H.L. Hernandez, E.A. Appel, Injectable liposome-based supramolecular hydrogels for the programmable release of multiple protein drugs, Matter. (2022), https://doi.org/10.1016/j.matt.2022.03.001.
[12] S.M.A. Halder, B. Sa, Entrapment efficiency and release characteristics of polyethyleneimine-treated or - untreated calcium alginate beads loaded with propranolol–resin complex, Int. J. Pharm. 302 (2005) 84–94.
[13] A. Bernkop-Schnürch, C.E. Kast, M.F. Richter, Improvement in the mucoadhesive properties of alginate by the covalent attachment of cysteine, J. Control. Release 71 (2001) 277–285.
[14] H. Cheng, Z. Cui, S. Guo, X. Zhang, Y. Huo, S. Mao, Mucoadhesive versus mucopenetrating nanoparticles for oral delivery of insulin, Acta Biomater. 135 (2021) 506–519.
[15] S. Bashyal, J.E. Seo, Y.W. Choi, S. Lee, Bile acid transporter-mediated oral absorption of insulin via hydrophobic ion-pairing approach, J. Control. Release 338 (2021) 644–661.
[16] X. Li, S. Guo, C. Zhu, Q. Zhu, Y. Gan, J. Rantanen, U.L. Rahbek, L. Hovgaard, M. Yang, Intestinal mucosa permeability following oral insulin delivery using core shell corona nanolipoparticles, Biomaterials. 34 (2013) 9678–9687.
[17] J. Li, H. Qiang, W. Yang, Y. Xu, T. Feng, H. Cai, S. Wang, Z. Liu, Z. Zhang, J. Zhang, Oral insulin delivery by epithelium microenvironment-adaptive nanoparticles, J. Control. Release 341 (2022) 31–43.
[18] L. Zhao, J. Ding, P. He, C. Xiao, Z. Tang, X. Zhuang, X. Chen, An efficient pH sensitive oral insulin delivery system enhanced by deoxycholic acid, J. Control. Release 152 (2011) 184–186.
[19] J. Li, H. Wu, K. Jiang, Y. Liu, L. Yang, H.J. Park, Alginate calcium microbeads containing chitosan nanoparticles for controlled insulin release, Appl. Biochem. Biotech. 193 (2021) 463–478.
[20] L.M. Hemmingsen, B. Giordani, A.K. Pettersen, B. Vitali, P. Basnet, N. Škalko-Basnet, Liposomes-in-chitosan hydrogel boosts potential of chlorhexidine in biofilm eradication in vitro, Carbohyd. Polym. 262 (2021), 117939, https://doi.org/10.1016/j.carbpol.2021.117939.
[21] E.J.B. Nielsen, S. Yoshida, N. Kamei, R. Iwamae, E.-S. Khafagy, J. Olsen, U. L. Rahbek, B.L. Pedersen, K. Takayama, M. Takeda-Morishita, In vivo proof of concept of oral insulin delivery based on a co-administration strategy with the cell-penetrating peptide penetratin, J. Control. Release 189 (2014) 19–24.
[22] N. Kamei, M. Morishita, Y. Eda, N. Ida, R. Nishio, K. Takayama, Usefulness of cell-penetrating peptides to improve intestinal insulin absorption, J. Control. Release 132 (2008) 21–25.
[23] S. Wang, X. Liu, I.J. Villar-Garcia, R. Chen, Amino acid based hydrogels with dual responsiveness for oral drug delivery, Macromol. Biosci. 16 (2016) 1258–1264.
[24] X. Qi, Y. Yuan, J. Zhang, J.W.M. Bulte, W. Dong, Oral administration of salecan-based hydrogels for controlled insulin delivery, J. Agr. Food. Chem. 66 (2018) 10479–10489.
[25] Z. Cui, L. Qin, S. Guo, H. Cheng, X. Zhang, J. Guan, S. Mao, Design of biotin decorated enterocyte targeting muco-inert nanocomplexes for enhanced oral insulin delivery, Carbohyd. Polym. 261 (2021), https://doi.org/10.1016/j.carbpol.2021.117873.
[26] S. Sudhakar, S.V. Chandran, N. Selvamurugan, R.A. Nazeer, Biodistribution and pharmacokinetics of thiolated chitosan nanoparticles for oral delivery of insulin in vivo, Int. J. Biol. Macromol. 150 (2020) 281–288.

[27] N.G. Hentz, J.M. Richardson, J.R. Sportsman, J. Daijo, G.S. Sittampalam, Synthesis and characterization of insulin–fluorescein derivatives for bioanalytical applications, Anal. Chem. 69 (1997) 4994–5000.
[28] A. Wang, T. Yang, W. Fan, Y. Yang, Q. Zhu, S. Guo, C. Zhu, Y. Yuan, T. Zhang, Y. Gan, Protein corona liposomes achieve efficient oral insulin delivery by overcoming mucus and epithelial barriers, Adv. Healthc. Mater. (2018), https://doi.org/10.1002/adhm.201801123.
[29] W. Fan, D. Xia, Q. Zhu, X. Li, S. He, C. Zhu, S. Guo, L. Hovgaard, M. Yang, Y. Gan, Functional nanoparticles exploit the bile acid pathway to overcome multiple barriers of the intestinal epithelium for oral insulin delivery, Biomaterials. 151 (2018) 13–23.
[30] O.M. Kolawole, L.W. Man, V.V. Khutoryanskiy, Methacrylated chitosan as a polymer with enhanced mucoadhesive properties for transmucosal drug delivery, Int. J. Biol. Macromol. 550 (2018) 123–129.
[31] L. Yin, J. Ding, C. He, L. Cui, C. Tang, C. Yin, Drug permeability and mucoadhesion properties of thiolated trimethyl chitosan nanoparticles in oral insulin delivery, Biomaterials. 30 (2009) 5691–5700.
[32] B. Bk, C. Ln, A. Py, E. Ehd, Characterization of arginine preventive effect on heat-induced aggregation of insulin, Int. J. Biol. Macromol. 145 (2020) 1039–1048.
[33] N. Kamei, E.S. Khafagy, J. Hirose, M. Takeda-Morishita, Potential of single cationic amino acid molecule "arginine" for stimulating oral absorption of insulin, Int. J. Pharm. 521 (2017) 176–183.
[34] M.K. Gök, K. Demir, E. Cevher, Y.L.Z. Özsoy, Ü. Cirit, S. Özgümüş, S. Pabuccuoğ, The effects of the thiolation with thioglycolic acid and l-cysteine on the mucoadhesion properties of the starch-graft-poly(acrylic acid), Carbohyd. Polym. 163 (2017) 129–136.
[35] J. Burana-Osot, N. Soonthornchareonnon, S. Hosoyama, R.J. Linhardt, T. Toida, Partial depolymerization of pectin by a photochemical reaction, Carbohydr. Res. 345 (2010) 1205–1210.
[36] Z. Özbaş, B. Özkahraman, Z.P. Akgüner, A. Bal-Öztürk, Evaluation of modified pectin/alginate buccal patches with enhanced mucoadhesive properties for drug release systems: In-vitro and ex-vivo study, J. Drug Deliv. Sci. Tec. 67 (2022) 102991, https://doi.org/10.1016/j.jddst.2021.102991.
[37] Y. Zhang, S. Zhou, F. Deng, X. Chen, X. Wang, Y. Wang, H. Zhang, W. Dai, B. He, Q. Zhang, The function and mechanism of preactivated thiomers in triggering epithelial tight junctions opening, Eur. J. Pharm. Biopharm. 133 (2018) 188–199.
[38] I.C. Carvalho, A. Mansur, S.M. Carvalho, R.M. Florentino, H.S. Mansur, L-cysteine and poly-L-arginine grafted carboxymethyl cellulose/Ag-In-S quantum dot fluorescent nanohybrids for in vitro bioimaging of brain cancer cells, Int. J. Biol. Macromol. 133 (2019) 739–753.
[39] B. Ye, L. Meng, Z. Li, R. Li, L. Li, L. Lu, S. Ding, J. Tian, C. Zhou, A facile method to prepare polysaccharide-based in-situ formable hydrogels with antibacterial ability, Mater. Lett. 183 (2016) 81–84.
[40] E. Moens, M. Veldhoen, Epithelial barrier biology: good fences make good neighbours, Immunology. 135 (2012) 1–8.
[41] L.R. Volpatti, M.A. Matranga, A.B. Cortinas, D. Delcassian, D.G. Anderson, Glucose-responsive nanoparticles for rapid and extended self-regulated insulin delivery, ACS Nano 14 (2019) 488–497.
[42] T. Zhang, J.Z. Tang, X. Fei, Y. Li, Y. Song, Z. Qian, Q. Peng, Can nanoparticles and nano–protein interactions bring a bright future for insulin delivery? Acta Pharm. Sin. B 11 (2021) 651–667.
[43] R.A. Cone, Barrier properties of mucus, Adv. Drug Deliver. Rev. 61 (2009) 75–85.
[44] G. Chen, D. Li, Y. Jin, W. Zhang, L. Teng, C. Bunt, J. Wen, Deformable liposomes by reverse-phase evaporation method for an enhanced skin delivery of (+)-catechin, Drug Dev. Ind. Pharm. 40 (2014) 260–265.
[45] C. Pidgeon, S. McNeely, T. Schmidt, J.E. Johnson, Multilayered vesicles prepared by reverse-phase evaporation: liposome structure and optimum solute entrapment, Biochemistry-US. 26 (1987) 17–29.
[46] L.V. Chernomordik, M.M. Kozlov, Mechanics of membrane fusion, Nat. Struct. Mol. Biol. 15 (2008) 675–683.
[47] S. Simões, J.N. Moreira, C. Fonseca, N. Düzgüneş, M.C. Pedroso de Lima, On the formulation of pH-sensitive liposomes with long circulation times, Adv. Drug Deliver. Rev. 56 (2004) 947–965.
[48] S. Simões, V. Slepushkin, N. Düzgünes, M.C. Pedroso de Lima, On the mechanisms of internalization and intracellular delivery mediated by pH-sensitive liposomes, BBA-Biomembranes. 1515 (2001) 23–37.
[49] S. Sajeesh, K. Bouchemal, V. Marsaud, C. Vauthier, C.P. Sharma, Cyclodextrin complexed insulin encapsulated hydrogel microparticles: an oral delivery system for insulin, J. Control. Release 147 (2010) 377–384.
[50] K. Lähdesmäki, O.H.S. Ollila, A. Koivuniemi, P.T. Kovanen, M.T. Hyvönen, Membrane simulations mimicking acidic pH reveal increased thickness and negative curvature in a bilayer consisting of lysophosphatidylcholines and free fatty acids, BBA-Biomembranes. 1798 (2010) 938–946.
[51] V.K.B. Jan-Willem, A.W.C. Einerhand, H. Büller, D. Jan, The oligomerization of a family of four genetically clustered human gastrointestinal mucins, Glycobiology. 8 (1998) 67–75.
[52] S. Zhou, H. Deng, Y. Zhang, P. Wu, X. Wang, Thiolated nanoparticles overcome the mucus barrier and epithelial barrier for oral delivery of insulin, Mol. Pharm. 17 (2019) 239–250.
[53] E.-S. Khafagy, R. Iwamae, N. Kamei, M. Takeda-Morishita, Region-dependent role of cell-penetrating peptides in insulin absorption across the rat small intestinal membrane, AAPS J. 17 (2015) 1427–1437.
[54] B. Gupta, T.S. Levchenko, V.P. Torchilin, Intracellular delivery of large molecules and small particles by cell-penetrating proteins and peptides, Adv. Drug Deliver. Rev. 57 (2005) 637–651.
[55] N. Kamei, Y. Onuki, K. Takayama, M. Takeda-Morishita, Mechanistic study of the uptake/permeation of cell-penetrating peptides across a caco-2 monolayer and their stimulatory effect on epithelial insulin transport, J. Pharm. Sci. 102 (2013) 3998–4008.
[56] B. Upendra, D. Sindhu, K. Nagavendra, K. Wahid, Liposomal formulations in clinical use: an updated review, Pharmaceutics 9 (2017) 12–45.
[57] J.A. Zuris, D.B. Thompson, Y. Shu, J.P. Guilinger, J.L. Bessen, J.H. Hu, M. L. Maeder, J.K. Joung, Z.Y. Chen, D.R. Liu, Cationic lipid-mediated delivery of proteins enables efficient protein-based genome editing in vitro and in vivo, Nat. Biotechnol. 33 (2015) 73–80.